Hindawi Publishing Corporation
International Journal of Photoenergy
Volume 2012, Article ID 208987, 7 pages
doi:10.1155/2012/208987

Research Article

Synthesis and Photocatalytic Activity of TiO_X Powders with Different Oxygen Defects

Leini Wang,[1] Fei Lu,[1] and Fanming Meng[1,2,3]

[1] *Anhui Key Laboratory of Information Materials and Devices, School of Physics and Materials Science, Anhui University, Hefei 230039, China*
[2] *Department of Physics and Astronomy, University of Arkansas at Little Rock, Little Rock, AR 72204, USA*
[3] *Key Laboratory of Materials Modification by Laser, Ion and Electron Beams Dalian University of Technology, Ministry of Education, Dalian 116024, China*

Correspondence should be addressed to Fanming Meng, mrmeng@ahu.edu.cn

Received 10 February 2012; Revised 28 March 2012; Accepted 30 March 2012

Academic Editor: Weifeng Yao

The novel carbon- or chromium-doped TiO_X photocatalysts with different oxygen defects were synthesized by mechanochemical technique and heating process. The samples were characterized by X-ray diffraction, UV-vis spectrophotometer, and fluorescence spectrometer. Carbon and chromium species were incorporated into TiO_X crystal matrix. The mass fraction of Ti_7O_{13} in TiO_X photocatalysts could be tunable through carbon or chromium doping. The mass fraction of Ti_7O_{13} could be an indication of the degree of oxygen defects (the concentration of Ti^{3+}) in the TiO_X. The degree of oxygen defects increased for carbon doping, while the degree of oxygen defects decreased for chromium doping. The photocatalytic activity measurement results showed that photodegradation rate of methyl orange reached the maximum value with mass fraction of Ti_7O_{13} of about 66.93%, but the photodegradation rate decreased when mass fraction of Ti_7O_{13} is raised further. In addition, the origin of absorption in the visible spectral range for carbon-doped TiO_X as well as the effect of band gap on photocatalytic activity has also been discussed in this paper.

1. Introduction

Currently, extensive research has been carried out on oxide semiconductor photocatalysis in the conditions of aggravation of environmental pollution and resources shortage [1–5]. In this sense, semiconductor photocatalysis can change solar energy to electrical and chemical energy, drive redox reactions, degrade organic substance, and improve environment. As the leading candidate semiconductor photocatalyst, titania has attracted most attention due to its unique physicochemical properties, including good chemical stability, inexpensiveness, relatively good reactivity, and notoxicity [6, 7]. However, the large band gap (3.2ev) of titania allows it to absorb only the ultraviolet light, which seriously restricts its utilization efficiency for the solar photons. Furthermore, the low-quantum yield that results from high frequency of recombination of photoinduced current carriers limits its practical applications [8, 9]. Hence, significant efforts, including metal or nonmetallic ions doping [10, 11], semiconductor coupling [12], and deposition of noble metals [13], have been devoted to extend the spectral response region of titania and enhance its photocatalytic activity.

The photocatalytic activity of doped TiO_2 is a complex function of the dopant concentration [14], crystal structure [11], surface area [15], and lattice defects. Especially oxygen vacancies play an important role in photocatalytic efficiency of TiO_2 [16–18]. However, the photocatalyst of the TiO_X with oxygen defects was little reported in previous literatures.

In this paper, TiO_X powder including Ti_7O_{13} and TiO_2 was used as precursor. Carbon or chromium doping was used to control the degree of oxygen defects of samples. The photocatalytic activities dependence on the degree of oxygen defects was evaluated in terms of the photodegradation of methyl orange (MO) under UV light irradiation. Furthermore, a facile green synthetic route of C-doped TiO_X was

developed, which could provide an effective technique for industrial production due to its low cost.

2. Experimental

2.1. Preparation of Samples. The TiO_X powder and chromic oxide (Cr_2O_3) were purchased from Tianjin Guangfu Fine Chemical Research Institute, China. Glucose ($C_6H_{12}O_6$) was purchased from Tianjin Guangfu technology development Co. Ltd., China. All the reagents were of analytical grade purity and used without any further purification. Distilled water was used in all experiments. A planetary ball mill was used for sample synthesis.

Carbon- and chromium-codoped TiO_X sample was prepared by following process. Appropriate amount of $C_6H_{12}O_6$ and Cr_2O_3 were added to TiO_X powder. The mass ratio of $Cr_2O_3/C_6H_{12}O_6/TiO_X$ was kept constant at 2 : 9 : 200. Total 40 g of above mixture was put into the bottle, and then 25 mL distilled water was added. After being milled for 180 min at a speed of 400 rpm, the wet powder was dried in air over at 90°C for 10 h. The ground powder was subsequently heated at 200°C for 300 min. The prepared catalyst was named C/Cr-TOV. Carbon-doped and chromium-doped and pure TiO_X samples were also prepared through the same method, without adding the corresponding dopant, named as C-TOV, Cr-TOV, and TOV, respectively. Namely, for the synthesis of Carbon-doped TiO_X, the mass ratio of $C_6H_{12}O_6/TiO_X$ was kept constant at 9 : 200. Total 40 g of above mixture was put into the bottle followed by the addition of 25 mL of distilled water.

2.2. Characterizations. The crystal phases of the samples were analyzed by X-ray diffraction (XRD) with CuKα. The crystalline sizes of anatase and Ti_7O_{13} were calculated by Scherrer formula. The average crystalline size was obtained using following equation [15]:

$$D_{\text{ave}} = D_a\left(\frac{I_a}{I_a + I_v}\right) + D_v\left(\frac{I_v}{I_a + I_v}\right), \quad (1)$$

where D_{ave} is average crystalline size, D_a and D_v are crystalline sizes of anatase and Ti_7O_{13}, respectively. I_a and I_v are peak intensity of anatase (1 0 1) and Ti_7O_{13} ($\bar{1}$ 2 5), respectively.

The mass fraction of anatase (W_a), Ti_7O_{13} (W_v), and brookite (W_b) were calculated using following equations [11, 19]:

$$W_a = \frac{I_a}{k_a^a\left((I_a/k_a^a) + (I_v/k_a^v) + (I_b/k_a^b)\right)}, \quad (2)$$

$$W_v = \frac{I_v}{k_a^v\left((I_a/k_a^a) + (I_v/k_a^v) + (I_b/k_a^b)\right)}, \quad (3)$$

$$W_b = \frac{I_b}{k_a^b\left((I_a/k_a^a) + (I_v/k_a^v) + (I_b/k_a^b)\right)}, \quad (4)$$

where I_a, I_v, and I_b are peak intensity of anatase (1 0 1), Ti_7O_{13} ($\bar{1}$ 2 5), and brookite (2 1 1), respectively. k_a^a, k_a^v, and k_a^b are constant (taken as 1, 0.1963, and 0.3354, resp.).

The UV-vis absorption spectroscopy of the sample was measured using Ultraviolet-Visible-Near Infrared Spectrophotometer (U-4100), while $BaSO_4$ was used as a reference. Photoluminescence (PL) spectra were obtained using a fluorescence spectrophotometer (F-4500) at room temperature.

2.3. Photocatalytic Activity. Photocatalytic activity of samples was characterized by decolorization of methyl orange (MO). The photocatalyst (0.3 g) was dispersed in 25 mL MO aqueous solution with a concentration of 5 ppm in a dish with diameter of 8 cm. The mixture was kept in the dark for 30 min to obtain the absorption-desorption equilibrium before UV-light irradiation. A 100 W mercury lamp was used as a light source. The distance between the lamp and the reaction solution was 9 cm. The absorbance of MO solution at 464 nm was measured with UV-vis spectrophotometer at intervals of 15 min and the total irradiation time was 45 min.

3. Results and Discussion

Figure 1 (a, b, c, d) shows the XRD patterns of the samples. It is found that all the samples consist of mixed phases of anatase, Ti_7O_{13}, and brookite. For doped TiO_X (b, c, d), the characteristic peaks of carbon and Cr_2O_3 are not observed. It may be attributed to the small amount of dopant or carbon, and Cr_2O_3 is dispersed uniformly into the TiO_X matrix [20, 21]. The average crystalline sizes of the samples and the mass fraction of three phases are calculated by equations (1)–(4), as listed in Table 1. As can be seen from Table 1, the average crystalline sizes of doped TiO_X are lower than that of undoped TiO_X.This result implies that the existence of impurity prevents the agglomeration of particles [15]. The samples show different mass fraction of three phases for different doping. Especially the mass fraction of Ti_7O_{13} is changed through carbon and Cr_2O_3 doping, which suggested that carbon or chromium doping can change the degree of oxygen defects for samples. This is because that the mass fraction of Ti_7O_{13} can be an indication of the degree of oxygen defects (the concentration of Ti^{3+}) in the TiO_X.

From Figure 1 (e, f, g, h), it can be seen that, compared with TOV, anatase peaks (1 0 1) and Ti_7O_{13} peaks ($\bar{1}$ 2 5) of other samples shift to lower 2θ value, which imply that the d-spacing of TiO_X increases. Furthermore, it is suggested that some of C/Cr atoms or ions have entered into the interstitial sites of TiO_X host and that results in the expansion of TiO_X lattice [20, 22].

Figure 2 shows the UV-vis absorption spectra of all the samples. In contrast to the pure TiO_X, carbon- or chromium-modified TiO_X show, broader absorption shoulders in the visible light region. The relation between absorption coefficient (α) and band gap (E_g) can be written as $(\alpha h\nu)^{1/2} \propto h\nu\text{-}E_g$, where ν is the frequency and h is Planck's constant [14]. The band gap energies can be estimated by the plot of $(\alpha h\nu)^{1/2}$ versus photon energy ($h\nu$), as shown in Figure 3 and listed in Table 1. It can be seen that the band gap for carbon- or Cr_2O_3-doped TiO_X is less than that of undoped TiO_X. Two small absorption peaks located at 450

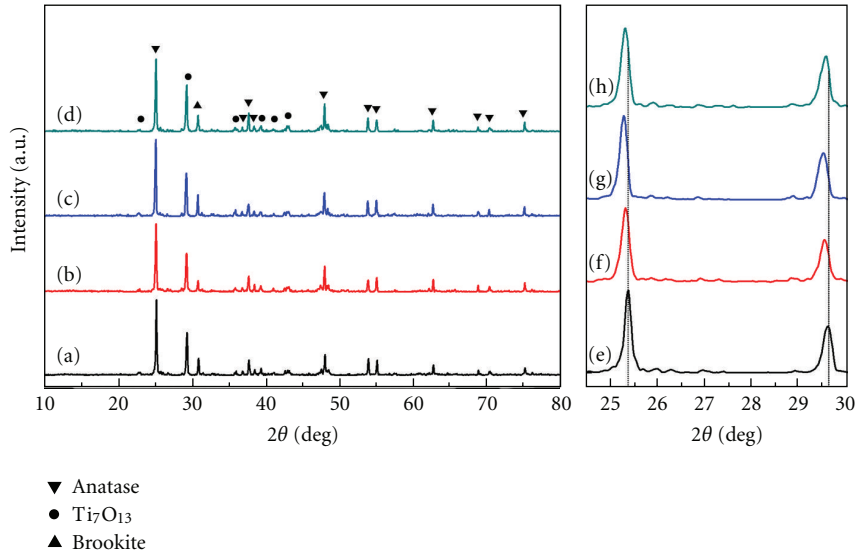

Figure 1: XRD patterns of samples with different oxygen defects: (a) undoped TiO_X, (b) C-doped TiO_X, (c) Cr-doped TiO_X, and (d) C/Cr-doped TiO_X. (e)–(h) are magnified XRD spectra of (a)–(d), respectively.

Table 1: Physicochemical properties of the TiO_X samples.

Samples	Crystalline Size (nm)	Anatase (wt %)	Ti_7O_{13} (wt %)	Brookite (wt %)	Band gap (eV)
TOV	42.3	20.01	66.93	13.06	3.13
Cr-TOV	40.5	19.79	66.87	13.34	3.09
C-TOV	38.4	22.02	67.73	10.25	3.02
C/Cr-TOV	38.5	18.41	68.19	13.40	2.99

and 600 nm can be observed clearly for Cr-TOV. Based on related documents [11, 23, 24], the peak located around 450 nm can be attributed to the charge transfers band $Cr^{3+} \rightarrow Ti^{4+}$ or $^4A_{2g} \rightarrow {}^4T_{1g}$ of Cr^{3+} in an octahedral environment, another due to $^4A_{2g} \rightarrow {}^4T_{2g}$ d-d transitions of Cr^{3+}. However, in the case of carbon-doped TiO_2, there is controversial reports in the literature for the origin of absorption in the visible spectral range. Some researchers proposed that this red shift was ascribed to the presence of localized states of the dopants in the band gap [14, 25]. While others have suggested that the formation of oxygen vacancies and the appearance of color centers were responsible for obvious absorption in the visible light range for nonmetal doped titania [16, 26]. It is well known that carbon atoms or ions that diffused into the interstitial sites of TiO_X host will "plunder" oxygen in TiO_X attributed to the chemical bond strength of C–O (1076 kJ/mol) stronger than that of Ti–O (662 kJ/mol) [21]. Oxygen vacancies state between the conduction and valence bands will be easier to form in the carbon-doped TiO_X [16]. We assume that carbon doping is consistent with the increase of oxygen vacancies that result in red shift for C-TOV and C/Cr-TOV. Similar results have been observed in nonmetal doped TiO_2 [20, 27, 28].

PL spectrum analysis is an effective tool to discern defect-related transitions in the samples. To further explore the degree of oxygen defects in the samples, PL measurements were done for all of the samples. Figure 4(a) shows the PL

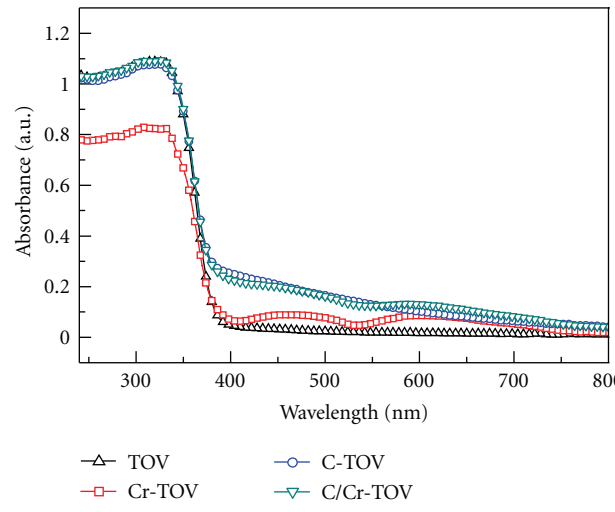

Figure 2: UV-vis absorption spectra of the samples with different oxygen defects.

spectra of TOV and Cr-TOV measured at room temperature at an excitation wavelength of 320 nm. It is found that the emission peaks are mainly centered on 400, 470, and 530 nm. The emission peaks around 400 nm are related to the band-edge free excitons. Peaks around 470 and

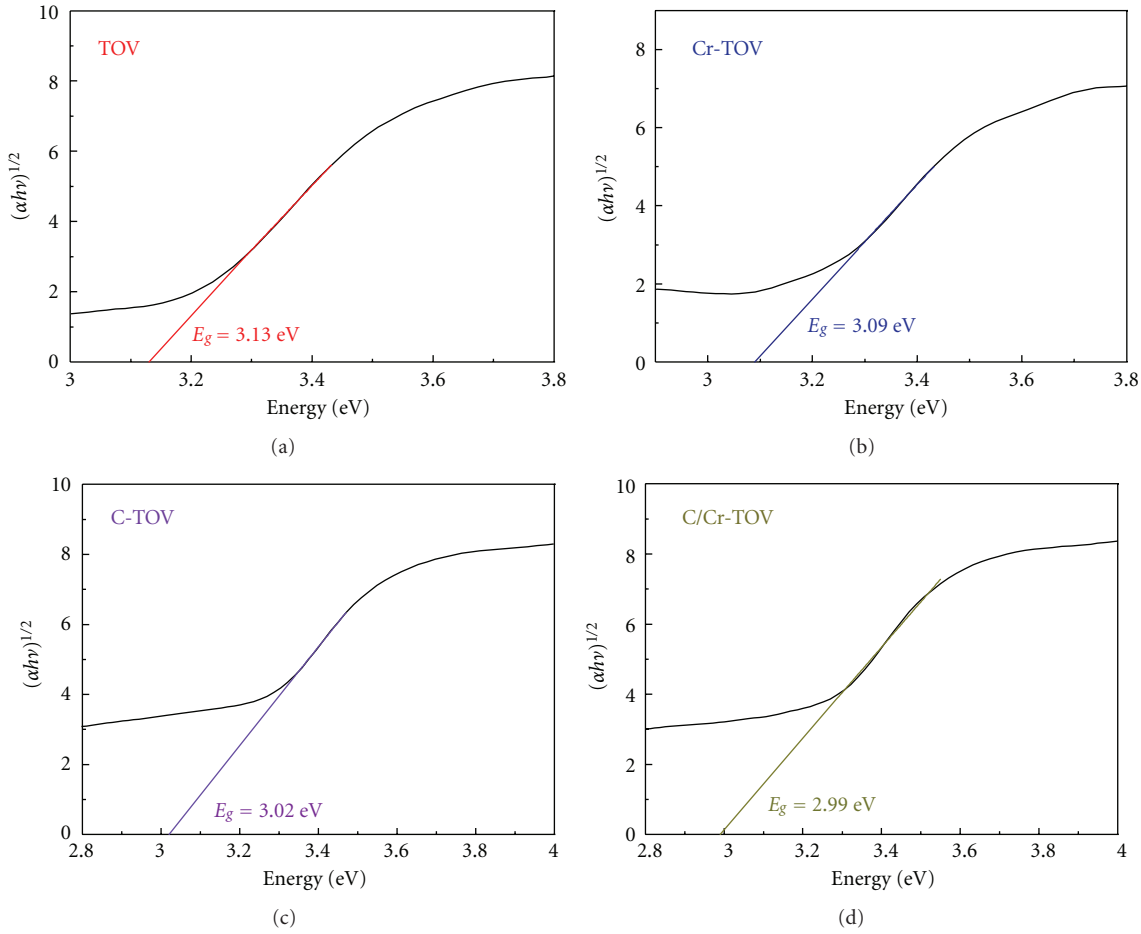

FIGURE 3: The plot of $(\alpha h\nu)^{1/2}$ versus photon energy of the samples with different oxygen defects.

530 nm originate from the bound excitons [29, 30]. The luminescence bands ranging from 460 to 580 nm for TiO_2 sample are ascribed to the transition from different exciton energy levels arising from oxygen vacancies to the valence band [29–31]. Obviously, the emission intensity increases with the degree of oxygen defects. Compared with the Cr-TOV sample, the enhanced PL intensity for TOV reflects the increases of the degree of oxygen defects in the TOV sample. The result is in good accord with the XRD analysis about the mass fraction of Ti_7O_{13} phase between TOV and Cr-TOV (Table 1). Also, it can be concluded from Figure 4(b) that the degree of oxygen defects of C/Cr-TOV is more than that of C-TOV. Combined with the XRD analysis, it is believed that the degree of oxygen defects of the samples is determined in the following order: C/Cr-TOV > C-TOV > TOV > Cr-TOV.

Figure 5 shows the reaction constant k for MO photodegradation of samples under UV light irradiation. The reaction constant is evaluated by equation: $\ln(C_0/C) = kt$ [32], where C_0 and C are the initial concentration and the reaction concentration of MO, t is the time of light irradiation. It is clear that the samples with different oxygen defects exhibit the superior photocatalytic activity compared with blank sample (the absence of photocatalyst) for decolorization rate of MO. In addition, the k is 0.135, 0.112, 0.104, and 0.081 for TOV, Cr-TOV, C-TOV, and C/Cr-TOV, respectively. Obviously, the loss of oxygen plays a significant role in improving the photodegradation rate for various catalysts.

The $\ln(C_0/C)$ dependence of the mass fraction of Ti_7O_{13} phase in the samples is showed in Figure 6. The mass fraction of Ti_7O_{13} can be an indication of the degree of oxygen defects (the concentration of Ti^{3+}) in the TiO_X. As can be seen from Figure 6, the photocatalytic activity increases and then decreases with the increase of the mass fraction of Ti_7O_{13}. The photocatalytic reaction rate of MO reaches the maximum value with mass fraction of Ti_7O_{13} of about 66.93%. The relationship between the decolorization of MO and the degree of oxygen defects (the concentration of Ti^{3+}) can be explained as follows. For TOV sample, appropriate degree of oxygen defects (or appropriate concentration of Ti^{3+}) would act as electron-trapping centers, which inhibit the recombination of photoinduced electron-hole pairs. And thus more photoinduced holes are removed to the surface of photocatalyst to produce more hydroxyl radicals and participate in the redox reaction that results in the enhancement of photocatalytic activity [17, 20, 26]. For Cr-TOV sample, lower concentration of oxygen defects (or lower concentration of Ti^{3+}) will lead to higher photocatalytic

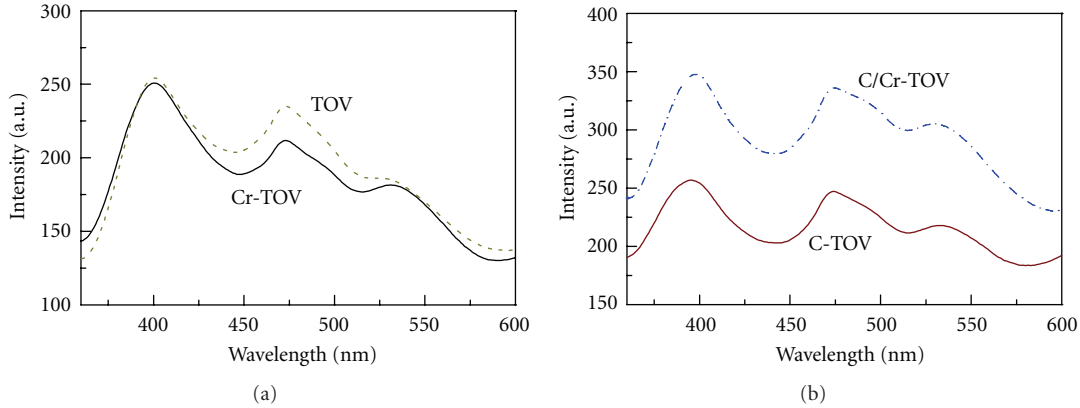

Figure 4: Photoluminescence spectra of samples: (a) TOV and Cr-TOV, (b) C/Cr-TOV and C-TOV at room temperature (λ_{ex} = 320 nm).

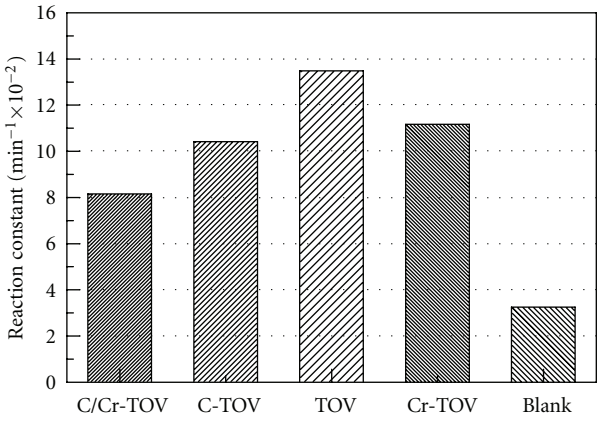

Figure 5: The comparison of reaction constant of different samples.

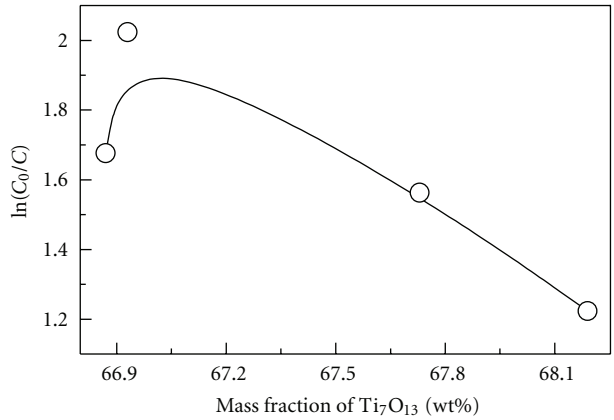

Figure 6: The photocatalytic activity as a function of the mass fraction of Ti_7O_{13}.

activity. However, in the case of C-TOV and C/Cr-TOV samples, the highest degree of oxygen defects (or the highest concentration of Ti^{3+}) results from carbon doping that suppresses the photocatalytic activity. This is because excess amount of oxygen vacancies would become recombination centers of the photoinduced charge carriers, leading to the depressed quantum yield [20].

In addition, there are also many factors [3] such as phase structure, band gap, and surface state that affect the photocatalytic activity. Combining absorption spectra analysis (band gap) with photocatalysis mechanism, photocatalytic activity of TiO_X is also dependent on energy gap. From above band gap of Table 1, it can be reasonably deduced that proper band gap (around 3.13 eV) is beneficial to creation of electronic-hole pairs that make excellent photocatalytic activity of TiO_X. When energy gap is smaller than 3.13 eV, it is beneficial to creation of electronic-hole pairs, but at the same time, recombination chance of electronic-hole increases, as a result, photocatalytic activity is lower.

4. Conclusions

In summary, some of C/Cr atoms or ions are successfully incorporated into the TiO_X host by mechanochemical and heating process. The mass fraction of Ti_7O_{13} phase of samples can be changeable by C/Cr doping. The mass fraction of Ti_7O_{13} increased for carbon- doping, while the mass fraction of Ti_7O_{13} decreased for chromium doping. The photocatalytic activity of samples is closely related to the degree of oxygen defects (the concentration of Ti^{3+}) and band gap. However, the photodegradation rate will be suppressed with excess oxygen defects. Furthermore, carbon doped TiO_X shows a broader absorption shoulder in the visible light region. It is attributed to the increase of oxygen vacancies and the advent of color centers.

Acknowledgments

This work was supported by the Natural Science Foundation of Anhui province of China (no. 1208085ME81), the Scientific Research Foundation of Education Ministry of Anhui province of China (nos. KJ2011A010 and KJ2012A029), the Teaching Research Foundation of Education Ministry of Anhui province of China (no. 20100185), the Doctor Scientific Research Starting Foundation of Anhui University

of China, the Foundation of "211 Project" of Anhui University of China (no. KJTD004B), and the Foundation of Construction of Quality Project of Anhui University of China (nos. XJ200907, xj201140, and 39020012).

References

[1] M. R. Hoffmann, S. T. Martin, W. Choi, and D. W. Bahnemann, "Environmental applications of semiconductor photocatalysis," *Chemical Reviews*, vol. 95, no. 1, pp. 69–96, 1995.

[2] F. M. Meng and F. Lu, "ure and silver (2.5–40 vol%) modified TiO_2 thin films deposited by radio frequency magnetron sputtering at room temperature: surface topography, energy gap and photo-induced hydrophilicity," *Journal of Alloys and Compounds*, vol. 501, no. 1, pp. 154–158, 2010.

[3] F. Meng and F. Lu, "Characterization and photocatalytic activity of TiO_2 thin films prepared by RF magnetron sputtering," *Vacuum*, vol. 85, no. 1, pp. 84–88, 2010.

[4] A. Fujishima and K. Honda, "Electrochemical photolysis of water at a semiconductor electrode," *Nature*, vol. 238, no. 5358, pp. 37–38, 1972.

[5] F. M. Meng, L. Xiao, and Z. Q. Sun, "Thermo-induced hydrophilicity of nano-TiO_2 thin films prepared by RF magnetron sputtering," *Journal of Alloys and Compounds*, vol. 485, no. 1-2, pp. 848–852, 2009.

[6] M. Ksibi, S. Rossignol, J. M. Tatibouët, and C. Trapalis, "Synthesis and solid characterization of nitrogen and sulfur-doped TiO_2 photocatalysts active under near visible light," *Materials Letters*, vol. 62, no. 26, pp. 4204–4206, 2008.

[7] W. Wang, J. Zhang, F. Chen, D. He, and M. Anpo, "Preparation and photocatalytic properties of Fe^{3+}-doped Ag@TiO_2 core-shell nanoparticles," *Journal of Colloid and Interface Science*, vol. 323, no. 1, pp. 182–186, 2008.

[8] H. G. Yu, S. C. Lee, J. G. Yu, and C. H. Ao, "Photocatalytic activity of dispersed TiO_2 particles deposited on glass fibers," *Journal of Molecular Catalysis A*, vol. 246, no. 1-2, pp. 206–211, 2006.

[9] J. G. Yu, G. H. Wang, B. Cheng, and M. H. Zhou, "Effects of hydrothermal temperature and time on the photocatalytic activity and microstructures of bimodal mesoporous TiO_2 powders," *Applied Catalysis B*, vol. 69, no. 3-4, pp. 171–180, 2007.

[10] H. Wang, Z. Wang, and Y. Liu, "A simple two-step template approach for preparing carbon-doped mesoporous TiO_2 hollow microspheres," *Journal of Physical Chemistry C*, vol. 113, no. 30, pp. 13317–13324, 2009.

[11] J. Choi, H. Park, and M. R. Hoffmann, "Effects of single metal-ion doping on the visible light photoreactivity of TiO_2," *The Journal of Physical Chemistry C*, vol. 114, pp. 783–792, 2010.

[12] W. Ho, J. C. Yu, J. Lin, J. Yu, and P. Li, "Preparation and photocatalytic behavior of MoS_2 and WS_2 nanocluster sensitized TiO_2," *Langmuir*, vol. 20, no. 14, pp. 5865–5869, 2004.

[13] L. L. Ren, Y. P. Zeng, and D. L. Jiang, "Preparation, characterization and photocatalytic activities of Ag-deposited porous TiO_2 sheets," *Catalysis Communications*, vol. 10, no. 5, pp. 645–649, 2009.

[14] Y. M. Wu, J. L. Zhang, L. Xiao, and F. Chen, "Properties of carbon and iron modified TiO_2 photocatalyst synthesized at low temperature and photodegradation of acid orange 7 under visible light," *Applied Surface Science*, vol. 256, no. 13, pp. 4260–4268, 2010.

[15] I. C. Kang, Q. W. Zhang, S. Yin, T. Sato, and F. Saito, "Preparation of a visible sensitive carbon doped TiO_2 photo-catalyst by grinding TiO_2 with ethanol and heating treatment," *Applied Catalysis B*, vol. 80, no. 1-2, pp. 81–87, 2008.

[16] V. N. Kuznetsov and N. Serpone, "On the origin of the spectral bands in the visible absorption spectra of visible-light-active TiO_2 specimens analysis and assignments," *Journal of Physical Chemistry C*, vol. 113, no. 34, pp. 15110–15123, 2009.

[17] P. Sangpour, F. Hashemi, and A. Z. Moshfegh, "Photoenhanced degradation of methylene blue on cosputtered M:TiO_2 (M = Au, Ag, Cu) nanocomposite systems: a comparative study," *Journal of Physical Chemistry C*, vol. 114, no. 33, pp. 13955–13961, 2010.

[18] Y. Z. Li, D. S. Hwang, N. H. Lee, and S. J. Kim, "Synthesis and characterization of carbon-doped titania as an artificial solar light sensitive photocatalyst," *Chemical Physics Letters*, vol. 404, no. 1–3, pp. 25–29, 2005.

[19] R. A. Spurr and H. Myers, "Quantitative analysis of anatase-rutile mixtures with an X-ray diffractometer," *Analytical Chemistry*, vol. 29, no. 5, pp. 760–762, 1957.

[20] Y. M. Wu, M. Y. Xing, J. L. Zhang, and F. Chen, "Effective visible light-active boron and carbon modified TiO_2 photocatalyst for degradation of organic pollutant," *Applied Catalysis B*, vol. 97, no. 1-2, pp. 182–189, 2010.

[21] J. Zhang, Z. Zhao, X. Wang et al., "Increasing the oxygen vacancy density on the TiO_2 surface by La-doping for dye-sensitized solar cells," *Journal of Physical Chemistry C*, vol. 114, no. 43, pp. 18396–18400, 2010.

[22] Y. W. Ma, J. Ding, J. B. Yi, H. T. Zhang, and C. M. Ng, "Mechanism of room temperature ferromagnetism in ZnO doped with Al," *Journal of Applied Physics*, vol. 105, no. 7, Article ID 07C503, 3 pages, 2009.

[23] J. F. Zhu, Z. G. Deng, F. Chen, J. L. Zhang, and H. J. Chen, "Hydrothermal doping method for preparation of Cr^{3+}-TiO_2 photocatalysts with concentration gradient distribution of Cr^{3+}," *Applied Catalysis B*, vol. 62, no. 3-4, pp. 329–335, 2006.

[24] X. X. Fan, X. Y. Chen, S. P. Zhu et al., "The structural, physical and photocatalytic properties of the mesoporous Cr-doped TiO_2," *Journal of Molecular Catalysis*, vol. 284, no. 1-2, pp. 155–160, 2008.

[25] X. B. Chen and C. Burda, "The electronic origin of the visible-light absorption properties of C-, N- and S-doped TiO_2 nanomaterials," *Journal of the American Chemical Society*, vol. 130, pp. 5018–5019, 2008.

[26] N. Serpone, "Is the band gap of pristine TiO_2 narrowed by anion- and cation-doping of titanium dioxide in second-generation photocatalysts?" *Journal of Physical Chemistry B*, vol. 110, no. 48, pp. 24287–24293, 2006.

[27] Y. Wang, C. X. Feng, M. Zhang, J. J. Yang, and Z. J. Zhang, "Enhanced visible light photocatalytic activity of N-doped TiO_2 in relation to single-electron-trapped oxygen vacancy and doped-nitrogen," *Applied Catalysis B*, vol. 100, no. 1-2, pp. 84–90, 2010.

[28] Q. Xiao, J. Zhang, C. Xiao, Z. Si, and X. Tan, "Solar photocatalytic degradation of methylene blue in carbon-doped TiO_2 nanoparticles suspension," *Solar Energy*, vol. 82, no. 8, pp. 706–713, 2008.

[29] K. Das, S. N. Sharma, M. Kumar, and S. K. De, "Morphology dependent luminescence properties of Co doped TiO_2 nanostructures," *Journal of Physical Chemistry C*, vol. 113, no. 33, pp. 14783–14792, 2009.

[30] W. F. Zhang, M. S. Zhang, Z. Yin, and Q. Chen, "Photoluminescence in anatase titanium dioxide nanocrystals," *Applied Physics B*, vol. 70, pp. 261–265, 2000.

[31] L. D. Zhang and C. M. Mo, "Luminescence in nanostructured materials," *Nanostructured Materials*, vol. 6, no. 5–8, pp. 831–834, 1995.

[32] F. Dong, W. Zhao, Z. Wu, and S. Guo, "Band structure and visible light photocatalytic activity of multi-type nitrogen doped TiO_2 nanoparticles prepared by thermal decomposition," *Journal of Hazardous Materials*, vol. 162, no. 2-3, pp. 763–770, 2009.